



The design of push-pull substituted coronene molecules for optoelectronic applications

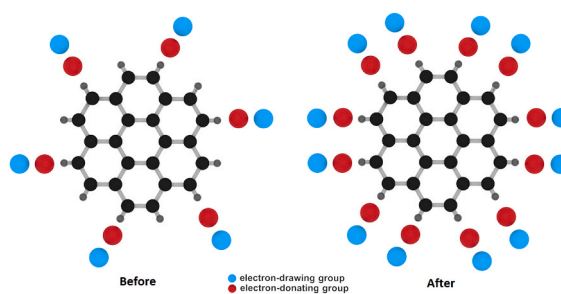
Cihan Demir, Ayhan Üngördü*

Department of Chemistry, Faculty of Science, Sivas Cumhuriyet University, 58140, Sivas, Turkey

HIGHLIGHTS

- Coronene and push-pull substituted coronene derivatives were theoretically designed for optoelectronic applications.
- The optoelectronic properties of the studied molecules were predicted using different computational chemistry tools.
- From the theoretically obtained results, suitable candidate(s) were suggested for each layer in OLED devices.

GRAPHICAL ABSTRACT



ARTICLE INFO

Keywords:

Push-pull substituted coronene
OLED
Computational approach
Organic electronic

ABSTRACT

The optoelectronic and electronic properties of coronene ([6]circulene) and push-pull coronene molecules were predicted by using different computational chemistry programs. For this aim, the electron/hole reorganization energies, the adiabatic/vertical ionization potentials, the adiabatic/vertical electron affinities, the chemical hardness values, the frontier orbital shapes and energy levels of the coronene and its derivatives were obtained at B3LYP/6-31G(d) level. Then the energies of the studied molecules in S_0 , S_1 , and T_1 states were calculated at PBE0/TZP level. From the obtained results, the emission values and TADF parameters of the investigated compounds were determined. Based on the theoretically obtained results, it was found that 6ethynyl-coronene and 12ethynyl-coronene molecules can be used as electron transfer materials and 6cyano-coronene and 12cyano-coronene compounds can be utilized as hole transfer materials. Additionally, it was noted that 6NO₂-coronene and 12NH₂-coronene derivatives can be good candidates for electron blocking materials, while 6NH₂-coronene and 12NH₂-coronene molecules can be utilized as hole blocking materials. Furthermore, it was emphasized that both 6NH₂-coronene and 12NH₂-coronene molecules can be good candidates as both electron injection and hole injection materials. Lastly, it was reported that 6ethynyl-coronene and 12cyano-coronene structures can be considered the most suitable candidates for near infrared organic emitting diodes.

1. Introduction

More than thirty years have passed since the discovery of the first

organic light emitting diode (OLED) from tris-(8-hydroxyquinoline) aluminum complex (Alq₃) by Tang and Van Slyke in 1987 [1]. During this time, enormous development of the OLED performance has been

* Corresponding author.

E-mail address: aungordu@cumhuriyet.edu.tr (A. Üngördü).

<https://doi.org/10.1016/j.matchemphys.2023.127631>

Received 30 September 2022; Received in revised form 31 January 2023; Accepted 12 March 2023

Available online 21 March 2023

0254-0584/© 2023 Elsevier B.V. All rights reserved.

achieved in terms of efficiency, color, and lifespan thanks to improvements in device engineering technology [2–7]. The efficiency has been quadrupled by developing OLED compounds that can convert singlet and triplet excitons into light [8,9]. The color quality has been tremendously improved by obtaining OLED molecules that emit high-purity red, green, and blue (RGB) light [10,11]. The lifespan has also been sufficiently extended for commercial use [12,13]. As a result of these developments combined with their light, flexible and thin structure, OLEDs have recently been widely used in small and large display screens [14–16]. While small sized-OLED panels are preferred for screens in smartphones, smartwatches, and portable gaming consoles, whereas large sized-OLED panels are used for high-performance displays in televisions, monitors, and signages [17–21]. After the widespread use of OLEDs, the discovery of new QLED devices has continued in recent years [22–24]. For instance, recently thermal activated delayed fluorescence (TADF) materials have been developed recently that can convert triplet excitons into light via reverse intersystem crossing (RISC) [25]. Addition to this, near infrared (NIR) OLED materials have been developed, which are used in important applications such as commutation networks, night vision devices and bioimaging, since their emission peak wavelengths are above 700 nm [26].

The circulenes are the macrocyclic arene in which a central n-sided polygon is surrounded and fused by benzenoids [27,28]. Nomenclature in this class of compounds is based on the number of benzene rings surrounding the core, which is equivalent to the size of the central polygon [29]. The optimized structures hydrocarbon [n]circulenes from the [3]circulene to [20]circulene were estimated by Hopf and coworkers using computational chemistry tools [30]. They have calculated the strain energy associated with the [n]circulenes compared to the energy related to [6]circulene (coronene). From strain energies, they have determined that the coronene structure is the most stable structure. Moreover, coronene can be imagined as the smallest graphite sheet and it are completely delocalized among the seven peri-fused aromatic benzene rings [31,32]. In addition, coronene compounds can be stacked closely in parallel with its adjacent molecule due to their unique flat structure, allowing excellent self-assembly and increased mobility of electrons [33,34]. Therefore, it can be considered as an important building block that can be used in new optoelectronic structures as OLED devices. Incorporation of heteroatoms into the coronene molecules can be develop its optoelectronic properties [30,35]. As an alternative to this modification, substituted coronene derivatives with electron with-drawing and electron-donating groups can also be taken into account [36]. Because, it is well known that electron with-drawing and electron-donating groups can be change the optoelectronic or electronic properties of the compounds [36,37]. Additionally, the symmetry group of the coronene molecule is D_{6h} [29]. The high symmetry of the coronene compound causes fundamental restrictions in its

electronic and vibrational spectra [38]. One way to reduce high symmetry is to attach a substituent to the molecule. Thus, the degree of the symmetry-point group of the molecule can be reduced and the aforementioned spectra can be improved.

The density functional theory (DFT) is a method that has been widely used in recent years as it has a low calculation cost and greater accuracy and is compatible with experimental result [39–42]. Additionally, the DFT method gives reasonable results for numerous aromatic and/or conjugated molecules [43–47]. The partial aims of this study are (1) to optimize the structures of the neutral, cationic and anionic charged states; (2) to determine energies of the highest occupied (HOMO) and the lowest unoccupied (LUMO) molecular orbitals, and (3) to interpret the electron and hole reorganization energies of push-pull substituted coronene compounds given in Scheme 1 by DFT method with the help of computational chemistry tools.

2. Methods

All calculations were performed by different computational tools, which are Gaussian 16 [48], Amsterdam Density Functional (ADF) 2019 [49], and Schrödinger Suite 2021–2 [50] programs, in the vacuo.

In Gaussian program, the electron/hole reorganization energies, the adiabatic/vertical ionization potentials, the adiabatic/vertical electron affinities, and the chemical hardness values of the studied push-pull coronene molecules were obtained at B3LYP/6–31G(d) level. Addition to these calculations, the frontier orbital shapes, the lowest unoccupied molecular orbital (LUMO) energy levels, the highest occupied molecular orbital (HOMO) energy levels and energy gaps of the investigated compounds were achieved at the same level.

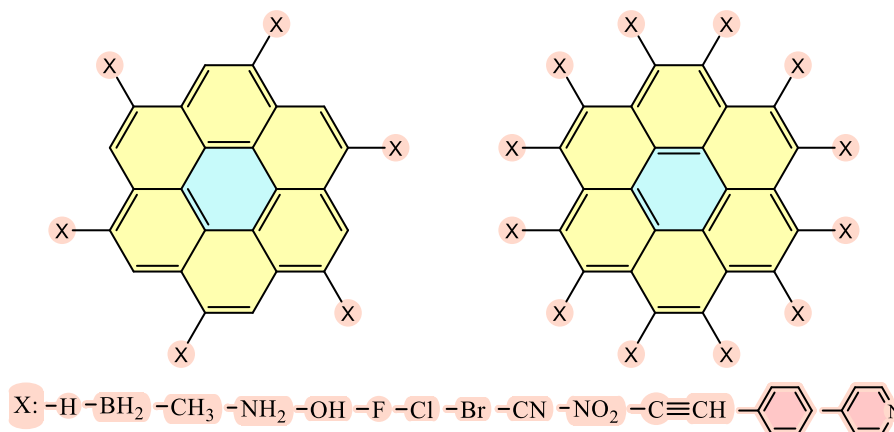
In ADF program, the energies of the coronene and substituted coronene molecules in S₀, S₁, and T₁ states were calculated at PBE0/TZP level because previous studies have indicated that PBE0 could be utilized as a good hybrid functional for emission computations [51]. From the results, the emission values and thermal activated delayed fluorescence (TADF) parameters of the studied molecules were computed.

In Schrödinger program, the reorganization energies, absorption/emission values and TADF parameters of the aforementioned compounds were calculated at B3LYP/MIDIXL level by using optimized structures obtained at B3LYP/6–31G(d) level in Gaussian program.

Charge transfer rates (k) of the molecules can be predicted using Marcus equation, expressed by Eq. (1) [52]:

$$k = \frac{4\pi^2 V^2 \exp(-\lambda/4k_B T)}{h \sqrt{4\pi\lambda k_B T}} \quad (1)$$

where V is the charge transfer integral, T is the absolute temperature, and λ is the reorganization energy which is sum of internal reorgani-



Scheme 1. Molecular structures of coronene and its derivatives discussed in this paper.

zation energy (λ_{int}) and external (λ_{ext}) reorganization energy. In addition to these descriptors, k_B and h are the Boltzmann and Planck constants, respectively. The charge-transfer rate of the compounds can be estimated by two key parameters, which are V and λ , at a certain temperature. To examine V , crystal data is generally needed. However, the designed molecules can be noncrystal, and the charge transfer integral is very limited. Therefore, to interpret the charge transfer rates of the studied molecules, their reorganization energies were taken into account. The reorganization energies are usually determined by a rapid change in molecular geometry when a charge is removed or added from compound (λ_{int}) and indicates the impact of enraptured medium on charge transfer (λ_{ext}). The λ_{ext} was ignored in the previous studies because there is an obvious correlation between λ_{int} and charge transfer rates. For that reason, it was focused on the debate of the λ_{int} to explain the charge transfer rates of the investigated compounds in this paper.

The reorganization energies (λ_s), the adiabatic/vertical ionization potentials (IPs), and the adiabatic/vertical electron affinities (EAs) can be calculated from single point energies via Eqs. (2)–(7) [53–55].

$$\lambda_e = (E_0^- - E_-^-) + (E_0^0 - E_0^0) \quad (2)$$

$$\lambda_h = (E_0^+ - E_+^+) + (E_0^0 - E_0^0) \quad (3)$$

$$IP_a = E_+^+ - E_0^0 \quad (4)$$

$$IP_v = E_0^+ - E_0^0 \quad (5)$$

$$EAA = E_0^0 - E_-^- \quad (6)$$

$$EAv = E_0^0 - E_0^- \quad (7)$$

where, $E_0^-(E_0^+)$ presents the energy of the anion (cation) obtained through the optimized neutral complex. Likewise, $E_-^-(E_+^+)$ stands for the energy of the anion (cation) calculated using the optimized anion (cation) structure, $E_0^-(E_0^+)$ defines the energy of the neutral compound computed at the anionic (cationic) state. E_0^0 also states the energy of the neutral molecule at the ground state.

In addition to the aforementioned descriptors, to estimate the stability of molecules, the absolute chemical hardness (η) [56] can be determined by the adiabatic ionization potential (IPa) and the electron affinity (EAA) by Eq. (8):

$$\eta = (IP_a - EAA) / 2 \quad (8)$$

All investigated molecules are closed-shell systems. The emission values of closed-shell systems can be predicted by utilizing the energy differences between ground-state energy (E_0) and the lowest excited-state energies (E_1) of the compounds via Eqs. (9) and (10):

$$\Delta E = E_1 - E_0 \quad (9)$$

$$\lambda = hc / \Delta E \quad (10)$$

here, ΔE and λ stands for the emission energy and wavelength, respectively. c is the light speed and h is Planck constant.

Finally, TADF performance of molecules are estimated with the help of Eq. (11) [57]:

$$\Delta E_{ST} = (ES_1 - ET_1) \quad (11)$$

where, ES_1 is the lowest-energy excited singlet state, while ET_1 is the lowest-energy excited triplet state.

3. Results and discussion

3.1. HOMO–LUMO analyses

Push-pull substituted coronene molecules are designed by attaching

6 or 12 electron-donating and electron-drawing groups to the coronene. Six-substituted coronene derivatives are labelled as 6X-coronene, whereas twelve-substituted coronene derivatives are presented as 12X-coronene. The studied coronene and push-pull substituted coronene compounds are optimized at B3LYP/6-31G(d) level and the optimized molecules are given in Tables S1 and S2. Additionally, Tables S1 and S2 show HOMO, LUMO shapes of the investigated molecules achieved at the same level. It is apparent from Tables S1 and S1, in the chemical systems substituted except for the systems having phenyl and 4-pyridyl substituents, it can be seen that frontier orbitals of the studied structures are also concentrated on the regions where substitutions are made. Addition to this, it can be said that HOMO and LUMO orbitals are delocalized on all molecules. On the other words, there is no the clear spatial separation of the frontier orbitals of the compounds. This situation causes to the obtaining of a high ΔE_{ST} for the investigated structures. Thus, it should be expected that all studied molecules will not be used as TADF materials.

On the other hand, the assessment of frontier molecular orbital energy levels is useful to estimate OLED behaviors because it has been reported that the HOMO and LUMO energy levels of molecules play an important role in OLED performance [58]. According to the report, higher exciton recombination occurs when the energy barrier between OLED layers is lower than 0.4 eV. Additionally, the LUMO levels of the molecules in the layer play a more important role than its HOMO levels in the governance of exciton recombination. To product high-performance OLEDs, particularly the differences between the LUMO values of the molecules located next to each other in the OLED layers should be considered. For that reason, the HOMO and LUMO energy levels of the studied compounds are also calculated at the B3LYP/6-31G(d) level and the obtained results are presented in Tables 1 and 2.

Within the framework of the HOMO and LUMO values given in Tables 1 and 2, the high-performance OLED structure consisting of the studied coronene and substituted coronene molecules can be designed. For instance, 6OH-coronene and 6phenyl-coronone compounds can be found in adjacent layers because their LUMO energy difference is 0.03 eV or 12Cl-coronene and 12Br-coronone molecules can be found in adjacent layers because their LUMO energy difference is 0.01 eV.

3.2. Reorganization energies

Reorganization energies, which are electron and hole reorganization energies, play a significant role in material efficacy for optoelectronic devices such as OLEDs. In the scope of Marcus theory, it is well-known that a small reorganization energy facilitates acceleration of the intermolecular charge hopping rate and develops the emission quantum yield for intramolecular excitations by decreasing the nonradiative decay rate. Therefore, the electron and hole reorganization energies of the studied coronene and substituted coronene derivatives are calculated at the B3LYP/6-31G(d) level and are given in Tables 1 and 2 Referring to Table 1, it can be shown that the electron reorganization energies of all compounds except for 6NH₂-coronene, 6OH-coronene, and 6NO₂-coronene derivatives are higher that of standard electron transport materials (ETL) which is AlQ3 ($\lambda_e = 0.276$) [59]. Therefore, the investigated compounds except for 6NH₂-coronene, 6OH-coronene, and 6NO₂-coronene derivatives can be proposed as ETL materials because of their low electron reorganization energies compared to the standard ETL compound. Moreover, it is can be said that the 6ethynyl-coronene derivative can be used as best ETL molecules among the studied all compounds. Considering the calculated hole reorganization energies from Table 1, it may be stated that the hole reorganization energies of all compounds except for 6NH₂-coronene and 6OH-coronene derivatives are higher that of standard hole transport materials (HTL) which is TPD ($\lambda_h = 0.290$) [60]. For that reason, these structures except for 6NH₂-coronene and 6OH-coronene molecules can be recommended as HTL molecules due to their low hole reorganization energies compared to the standard HTL

Table 1

The achieved computational chemical parameters (all in eV) of the studied 6X-coronene molecules at B3LYP/6-31G(d) level.

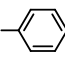
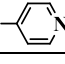
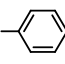
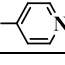
6X	HOMO	LUMO	λ_e	λ_h	IPa	IPv	EAa	EAv	η
-H	-5.45	-1.41	0.18	0.13	6.79	6.85	0.11	0.03	3.34
-BH ₂	-6.38	-2.96	0.16	0.18	7.52	7.61	1.86	1.79	2.83
-CH ₃	-5.18	-1.25	0.17	0.13	6.39	6.46	0.07	-0.02	3.16
-NH ₂	-4.42	-0.78	0.31	0.45	5.48	5.70	-0.35	-0.51	2.91
-OH	-5.23	-1.47	0.32	0.30	6.42	6.58	0.29	0.13	3.06
-F	-5.99	-2.02	0.23	0.20	7.29	7.39	0.75	0.63	3.27
-Cl	-6.28	-2.45	0.20	0.18	7.44	7.53	1.30	1.20	3.07
-Br	-6.21	-2.42	0.20	0.16	7.32	7.40	1.31	1.21	3.00
-CN	-7.44	-3.81	0.15	0.11	8.59	8.65	2.67	2.59	2.96
-NO ₂	-7.70	-4.14	0.36	0.20	8.85	8.95	3.11	2.92	2.87
-C≡CH	-5.66	-2.18	0.14	0.11	6.74	6.80	1.10	1.03	2.82
	-5.23	-1.50	0.22	0.18	6.16	6.25	0.60	0.49	2.78
	-6.00	-2.26	0.27	0.16	6.96	7.04	1.38	1.24	2.79

Table 2

The obtained computational chemical parameters (all in eV) of the studied 12X-coronene compounds at B3LYP/6-31G(d) level.

12X	HOMO	LUMO	λ_e	λ_h	IPa	IPv	EAa	EAv	η
-H	-5.45	-1.41	0.18	0.13	6.79	6.85	0.11	-0.09	3.34
-BH ₂	-6.05	-2.87	0.19	0.17	7.16	7.24	1.81	1.72	2.67
-CH ₃	-4.80	-1.16	0.21	0.18	5.91	6.00	0.08	-0.03	2.92
-NH ₂	-3.96	-0.58	0.56	0.54	4.90	5.18	-0.36	-0.64	2.63
-OH	-4.63	-1.09	0.31	0.29	5.79	5.94	-0.07	-0.22	2.93
-F	-6.35	-2.56	0.27	0.25	7.61	7.74	1.30	1.17	3.16
-Cl	-6.55	-3.18	0.26	0.21	7.59	7.70	2.16	2.03	2.72
-Br	-6.35	-3.09	0.25	0.18	7.34	7.42	2.14	2.01	2.60
-CN	-8.45	-5.31	0.16	0.11	9.49	9.54	4.29	4.21	2.60
-NO ₂	-8.73	-5.40	0.37	0.22	9.75	9.86	4.45	4.26	2.65
-C≡CH	-5.52	-2.59	0.14	0.11	6.48	6.54	1.64	1.57	2.42
	-5.09	-1.64	0.22	0.19	5.86	5.96	0.88	0.77	2.49
	-6.23	-2.80	0.26	0.17	7.05	7.13	2.03	1.90	2.51

material. In addition to this, one says that the 6ethynyl-coronene and 6cyano-coronene derivatives can be utilized as good HTL materials among the investigated all molecules. Taken into consideration calculated low electron and hole reorganization energies from Table 1, it is required to note that 6ethynyl-coronene and 6cyano-coronene molecules can be used as ambipolar material. Moreover, it is shown from Table 1 that the molecule having the highest electron reorganization energy (0.36 eV) is 6NO₂-coronene. Thus, it can be stated that 6NO₂-coronene can be proposed as an electron blocking layer (EBL) material because of its high λ_e value [61]. In addition, it is apparent from Table 1 that molecules with the highest hole reorganization energy (0.45 eV) is 6NH₂-coronene. Therefore, it can be stated that 6NH₂-coronene can be considered as hole blocking layer (HBL) materials due to their high λ_h values [61].

Considering reorganization energies given in Table 2, it is shown that the electron reorganization energies of 12X-coronene molecules are generally increased compared to those of 6X-coronene derivatives. Additionally, a trend similar to that of 6X-coronene is observed in reorganization energies taken into account. In other words, it can also be said from data given in Table 2 that the electron reorganization energies of all compounds except for 6NH₂-coronene, 6OH-coronene, and 6NO₂-coronene structures are higher than that of AlQ3. It can be noted from Table 2 that 12X-coronene molecules having lower electron reorganization energies from that of AlQ3 can be suggested as ETL materials and 12ethynyl-coronene molecule within these compounds can be used as the best ETL material. From hole reorganization energies given in Table 2, it can be noticed that the hole reorganization energies of all coronene structures except for 12NH₂-coronene molecule are higher

than that of TPD. Thus, all 12X-coronenes except for 12NH₂-coronene can be utilized as HTL materials owing to their lower hole reorganization energies compared to that of TPD. Furthermore, it can be stated that the 12ethynyl-coronene and 12cyano-coronene can be used as good HTL materials within the studied 12X-coronenes. Additionally, it is important to note that 12ethynyl-coronene and 12cyano-coronene molecules can be suggested as ambipolar material. It can also be seen from data given in Table 2 that the coronene derivative having the highest electron reorganization energy (0.56 eV) is 12NH₂-coronene. Thus, it can be said that 12NH₂-coronene can be considered as an electron blocking layer (EBL) material because of its high λ_e value [61]. In addition, it is obvious from Table 2 that substituted coronene with the highest hole reorganization energy (0.54 eV) is 12NH₂-coronene. Therefore, it can be stated that 12NH₂-coronene can be considered as hole blocking layer (HBL) materials due to their high λ_h values [61]. From the high reorganization energies, it should be noted that 12NH₂-coronene can be used as both EBL and HBL materials.

3.3. Ionization potentials and electron affinities

Ionization potentials and electron affinity values are useful descriptors used to estimate the materials in the injection layers of OLED structure. Therefore, the adiabatic/vertical ionization potential and the adiabatic/vertical electron affinity values of the studied coronene and push-pull coronene compounds are calculated at B3LYP/6-31G(d) level and the obtained results are tabulated in Tables 1 and 2. As shown in Table 1, the coronene derivative having the lowest ionization potential and electron affinity value is 6NH₂-coronene molecule. For that reason,

it can be said that 6NH₂-coronene can be used as a good electron injection layer (EIL) compound and a good hole injection layer (HIL) material [62]. Taken into account Table 2, it can be said that 12NH₂-coronene can be utilized as good EIL and HIL materials. As a result, one says that the amino group causes the coronene molecule to act as good EIL and HIL materials.

3.4. Chemical hardnesses

Chemical hardness value calculated from Koopmans' theorem is a useful quantum chemical parameter used in many theoretical studies [63]. In this study, it can be used to predict the stability of materials used in OLED layers. For that reason, the chemical hardness values of the coronene and coronene derivatives are computed at B3LYP/6-31G(d) level. The calculated chemical hardness values are given in Tables 1 and 2. Considering Tables 1 and 2, it is clearly seen that the compound with the highest hardness value is unsubstituted coronene. Thus, it can be stated that coronene is the most stable molecule among all the compounds studied. Addition to this, one can say that the investigated substituents reduce the stability of the coronene.

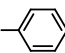
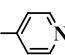
3.5. TADF performances

The absorption calculations of studied molecules are carried out at B3LYP/TZP level. From absorption spectra, the maximum oscillator strengths for S₀→S₁ transitions are determined and these values are given in Tables 3 and 4. Considering to Tables 3 and 4, it can be seen that the oscillator strengths of studied molecules are quite high. This means that the S₀→S₁ transition in all investigated compounds can be quite easy. From data given in Tables 3 and 4, it can be said that the π -conjugated substituents increase the oscillator strengths of coronene structure.

TADF OLED performance of molecules can be estimated from the energy difference between S₁ and T₁ levels in the compound. In addition, the S₁-T₁ value of compound must be less than 0.2 eV for efficient TADF OLED material. To estimate TADF OLED performance of the studied structures, the energies of the coronene and push-pull coronene structures in S₀, S₁, and T₁ states are calculated at PBE0/TZP level. The S₁-T₁ energy differences obtained through the calculations made are presented in Tables 3 and 4. Referring to Tables 3 and 4, it is obviously seen that the S₁-T₁ values of all studied compounds are considerably higher than the aforementioned reference value. Therefore, it can easily be said that the investigated coronene and coronene derivatives could not good candidate for TADF OLED materials.

Table 3

The oscillator strengths for S₀→S₁ transitions, the energy differences (eV) between the ground (S₀) and the singlet (S₁)/the triplet (T₁) states of the examined 6X-coronene molecules at B3LYP/TZP level and the emission wavelengths (nm) corresponding to these differences.

6X	$f_{(S_0 \rightarrow S_1)}$	S ₁ -S ₀	T ₁ -S ₀	S ₁ -T ₁	Fluorescence	Phosphorescence
-H	1.45	3.26	2.40	0.86	380	516
-BH ₂	0.67	2.81	2.10	0.71	442	591
-CH ₃	0.85	3.15	2.34	0.81	394	530
-NH ₂	0.74	2.92	2.21	0.71	425	562
-OH	0.72	3.06	2.28	0.77	406	543
-F	0.73	3.21	2.37	0.84	386	523
-Cl	0.83	3.05	2.23	0.82	406	556
-Br	0.86	3.04	2.24	0.81	407	555
-CN	0.90	2.95	2.12	0.84	420	586
-NO ₂	0.64	2.94	2.16	0.78	422	573
-C≡CH	0.98	2.82	2.01	0.81	440	618
	1.31	3.01	2.23	0.78	411	555
	1.23	3.02	2.24	0.78	410	553

3.6. NIR properties

Near-Infrared organic (carbon-based) light-emitting diodes (NIR OLEDs) are a class of OLEDs that emits light beyond 700 nm wavelength. For NIR OLED candidates, emission wavelength of the compound should be above 700 nm. From energy values calculated from geometries in S₀, S₁, and T₁ states, fluorescence and phosphorescence emission wavelengths are roughly determined and the obtained results are given in Tables 3 and 4. As shown in Table 3, the fluorescence and phosphorescence emission wavelengths of coronene are calculated as 380 and 516, respectively. Considering the effect of the substituents on the emission values, it can be said that all of the substituents examined show a bathochromic effect by increasing the aforementioned emission wavelengths of coronene. Despite the bathochromic effect, it is required to mention that the investigated 6X-coronene derivatives could not be candidate for NIR OLED materials because their emission values are below 700 nm. However, among the substituted coronene molecules, it can be said that the phosphorescence emission wavelengths of 6ethynyl-coronene molecule is near to infrared region. Referring to Table 4, it is seen that 12 substituents have a greater bathochromic effect on the emission of coronene than 6 substituents. From the emission values obtained in Table 4, it is shown that the phosphorescence emission wavelengths of 12cyano-coronene and 6ethynyl-coronene molecules among 12X-coronene compounds are in the NIR region. Based on these results, it can be stated that 12cyano-coronene and 6ethynyl-coronene derivatives can be proposed as NIR OLED materials.

3.7. A simple way to predict the OLED parameters

The computational cost of OLED descriptor in some computational chemistry software such as Gaussian and Amsterdam Density Functional programs are very high. For example, the seven energy values which are E_0^- , E_0^+ , E_1^- , E_1^+ , E_0^0 , E_1^0 , E_0^0 must be obtained for the calculation of the reorganization energies in Gaussian program or to find the energy difference between S₁ and T₁ levels is required to calculate the energies of the lowest-energy excited singlet and the lowest-energy excited triplet states in Amsterdam Density Functional program. In this study, a way has been proposed to reduce the cost of the calculations mentioned. Aforementioned OLED parameters can be easily calculated B3LYP/MIDIXL level in the Schrödinger program using the optimized structures obtained in the Gaussian program. This means that the calculation cost is considerably reduced. The results obtained from the compounds studied in this way are presented in Tables 5 and 6. In addition to the values obtained in other programs, absorption values are provided as well in the same table. When Table 5(6) is compared with Table 1 (2) and 3(4), it is clearly seen that the OLED parameters obtained in different

Table 4

The oscillator strengths for S₀→S₁ transitions, the energy differences (eV) between the ground (S₀) and the singlet (S₁)/the triplet (T₁) states of the investigated 12X-coronene structures at B3LYP/TZP level and the emission wavelengths (nm) corresponding to these differences.

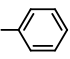
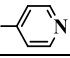
12X	f _(S₀→S₁)	S ₁ -S ₀	T ₁ -S ₀	S ₁ -T ₁	Fluorescence	Phosphorescence
-H	1.45	3.26	2.40	0.86	380	516
-BH ₂	1.22	2.59	1.95	0.64	479	637
-CH ₃	0.81	2.87	2.09	0.79	431	594
-NH ₂	0.74	2.68	1.96	0.72	463	634
-OH	0.76	2.89	2.12	0.78	428	585
-F	0.74	3.10	2.25	0.85	400	551
-Cl	1.45	2.63	1.91	0.72	472	651
-Br	0.64	2.54	1.82	0.71	488	680
-CN	0.88	2.57	1.74	0.83	483	714
-NO ₂	0.65	2.85	2.03	0.82	435	610
-C≡CH	1.78	2.35	1.59	0.76	527	778
	1.15	2.86	1.93	0.93	434	644
	1.17	2.92	1.95	0.97	424	635

Table 5

The obtained reorganization energies (eV), absorption wavelengths (nm), emission wavelengths (nm), and TADF parameters (eV) of the mentioned 6X-coronene molecules at B3LYP/MIDIXL level.

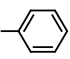
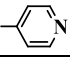
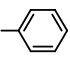
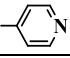
6X	λ _e	λ _h	L _{max}	E _{max}	S ₁ -T ₁
-H	0.12	0.16	280	396	0.81
-BH ₂	0.17	0.15	352	465	0.63
-CH ₃	0.13	0.16	292	408	0.77
-NH ₂	0.44	0.31	320	437	0.71
-OH	0.30	0.32	304	424	0.76
-F	0.19	0.22	286	402	0.80
-Cl	0.17	0.19	301	419	0.77
-Br	0.17	0.20	307	423	0.75
-CN	0.11	0.14	319	442	0.71
-NO ₂	0.21	0.19	348	453	0.69
-C≡CH	0.10	0.13	337	463	0.69
	0.17	0.21	321	438	0.74
	0.16	0.26	320	437	0.71

Table 6

The obtained reorganization energies (eV), absorption wavelengths (nm), emission wavelengths (nm), and TADF parameters (eV) of the mentioned 12X-coronene molecules at B3LYP/MIDIXL level.

12X	λ _e	λ _h	L _{max}	E _{max}	S ₁ -T ₁
-H	0.12	0.16	280	396	0.81
-BH ₂	0.15	0.18	382	507	0.58
-CH ₃	0.17	0.20	319	454	0.83
-NH ₂	0.51	0.54	345	484	0.69
-OH	0.29	0.29	318	449	0.73
-F	0.24	0.26	296	420	0.80
-Cl	0.21	0.26	352	495	0.76
-Br	0.17	0.28	380	518	0.74
-CN	0.09	0.14	369	518	0.63
-NO ₂	0.15	0.37	354	472	0.78
-C≡CH	0.11	0.13	407	564	0.62
	0.19	0.31	344	463	0.89
	0.17	0.26	337	459	0.89

computational programs are compatible. In this case, it is important to report that OLED descriptors can be easily obtained with the Schrödinger program using optimized structures because the mentioned way has low computational cost.

4. Conclusions

In this study, the coronene and push-pull substituted coronene molecules are theoretically designed via different computational chemistry tools. The optoelectronic and the electronic properties of the mentioned coronene molecules are estimated using quantum chemical descriptors. From theoretical obtained results, it can be said that 6ethynyl-coronene (or 12ethynyl-coronene) and 6cyano-coronene (or 12cyano-coronene) derivatives can be proposed as good candidates for ETL and HTL materials, respectively. Moreover, it can be stated that 6NO₂-coronene (or 12NH₂-coronene) and 6NH₂-coronene (or 12NH₂-coronene) derivatives can be predicted as good candidates for EBL and HBL compounds, respectively. Furthermore, it is required to note that both 6NH₂-coronene and 12NH₂-coronene molecules can be considered both EIL and HIL materials. Finally, it can be said from values given in related to tables that 6ethynyl-coronene and 12cyano-coronene structures can be suitable candidates for NIR OLED materials.

CRedit authorship contribution statement

Cihan Demir: Conceptualization, Methodology, Software, Validation, Formal analysis, Writing – original draft, Investigation, Writing – rrReview & e . **Ayhan Üngördü:** Conceptualization, Methodology, Software, Validation, Formal analysis, Writing – original draft, Investigation, Writing – rrReview & .

Declaration of competing interest

The authors declare that they have no known competing financial interests or personal relationships that could have appeared to influence the work reported in this paper.

Data availability

No data was used for the research described in the article.

Acknowledgements

The numerical calculations presented in this article were partially carried out at TUBITAK ULAKBIM, High Performance, and Grid Computing Center (TRUBA resources). In this study, the laboratory facilities of the Advanced Technology Application and Research Center of Sivas Cumhuriyet University (CÜTAM) were also used. This work is supported by the Scientific Research Project Fund of Sivas Cumhuriyet University under the project numbers F-2022-676.

Appendix A. Supplementary data

Supplementary data to this article can be found online at <https://doi.org/10.1016/j.matchemphys.2023.127631>.

References

- [1] C.W. Tang, S.A. VanSlyke, Organic electroluminescent diodes, *Appl. Phys. Lett.* 51 (1987) 913–915.
- [2] C.J. Zhou, Y.F. Liu, Z.Z. Sun, H. Liu, L. Xu, D.H. Hu, J. Hu, Efficient red hybridized local and charge-transfer OLEDs by rational isomer engineering, *Dyes Pigments* (2022) 205.
- [3] E. Witkowska, I. Glowacki, T.H. Ke, P. Malinowski, P. Heremans, Efficient OLEDs Based on Slot-Die-Coated Multi-Component Emissive Layer, 14, 2022. *Polymers-Basel*.
- [4] X.Y. Liu, J.W. Li, X. Qiu, X.Y. Ye, L. Xu, D.H. Hu, Highly efficient non-doped deep-blue OLED with NTSC CIEy and negligible efficiency roll-off based on emitter possessing hydrogen bond and hybridized excited state, *Dyes Pigments* 200 (2022).
- [5] Y.X. Fan, A.H. Sun, Y.H. Tian, P.C. Zhou, Y.X. Niu, W. Shi, B. Wei, Deep blue exciplex tandem OLEDs using n- and p-doped planar heterojunction as a charge generation layer, *J. Phys. D Appl. Phys.* 55 (2022).
- [6] Q.Y. Feng, K.S. Tan, X.J. Zheng, S.L. Xie, K. Xue, Y.F. Bo, H. Zhang, D.Q. Lin, J. F. Rao, X.M. Xie, L.H. Xie, H.T. Cao, H.M. Zhang, Y. Wei, W. Huang, Simultaneous and significant improvements in efficiency and stability of deep-blue organic light emitting diodes through friedel-crafts arylmethylation of a fluorophore, *Chemphotochem* 4 (2020) 321–326.
- [7] H.H. Kuo, Z.L. Zhu, G.S. Lee, Y.K. Chen, S.H. Liu, P.T. Chou, A.K.Y. Jen, Y. Chi, Bistridentate iridium(III) phosphors with very high photostability and fabrication of blue-emitting OLEDs, *Adv. Sci.* 5 (2018).
- [8] L.E. de Sousa, L.D. Born, P.H.D. Neto, P. de Silva, Triplet-to-singlet exciton transfer in hyperfluorescent OLED materials, *J. Mater. Chem. C* 10 (2022) 4914–4922.
- [9] S. Achelle, M. Hodee, J. Massue, A. Fihey, C. Katan, Diazine-based thermally activated delayed fluorescence chromophores, *Dyes Pigments* 200 (2022).
- [10] Y.H. Sun, X.L. Yang, Z. Feng, B.A. Liu, D.K. Zhong, J.J. Zhang, G.J. Zhou, Z.X. Wu, Highly efficient deep-red organic light-emitting devices based on asymmetric iridium(III) complexes with the thianthrene 5,5,10,10-tetraoxide moiety, *ACS Appl. Mater. Interfaces* 11 (2019) 26152–26164.
- [11] D.K. Dubey, R.K. Konidena, S. Sahoo, R.A.K. Yadav, S.S. Swayamprabha, K.R. J. Thomas, J.H. Jou, Wide color gamut deep-blue OLED architecture for display application, *Wide Bandgap Semicond. Mater.Devices* 19 85 (2018) 33–39.
- [12] R. Mac Ciarnain, H.W. Mo, K. Nagayoshi, H. Fujimoto, K. Harada, R. Gehlhaar, T. H. Ke, P. Heremans, C. Adachi, A thermally activated delayed fluorescence green OLED with 4500 h lifetime and 20% external quantum efficiency by optimizing the emission zone using a single-emission spectrum technique, *Adv. Mater.* 34 (2022).
- [13] S.H. Hu, Y.H. Tian, Y. Lin, W. Shi, Y.D. Pang, S.H. Pan, B. Wei, High-efficiency and Long-Lifetime Deep-Blue Organic Light-Emitting Diode with a Maximum External Quantum Efficiency of 20.6% and CIEy of 0.04, *Dyes Pigments*, 2022, p. 205.
- [14] A.K. Chauhan, P. Jha, D.K. Aswal, J.V. Yakhami, Organic devices: fabrication, applications, and challenges, *J. Electron. Mater.* 51 (2022) 447–485.
- [15] J. Bauri, R.B. Choudhary, G. Mandal, Recent advances in efficient emissive materials-based OLED applications: a review, *J. Mater. Sci.* 56 (2021) 18837–18866.
- [16] J.W. Park, D.C. Shin, S.H. Park, Large-area OLED lightings and their applications, *Semicond. Sci. Technol.* 26 (2011).
- [17] A.K. Sajeve, N. Agarwal, A. Soman, S. Gupta, M. Katiyar, A. Ajayaghosh, K.N. N. Unni, Enhanced light extraction from organic light emitting diodes using a flexible polymer-nanoparticle scattering layer, *Org. Electron.* 100 (2022).
- [18] W. Chen, C. Xu, L. Kong, X.Y. Liu, X. Zhang, N. Lin, X. Ouyang, Silk fibroin-based flexible organic light-emitting diode with high light extraction efficiency, *Adv. Opt. Mater.* 10 (12) (2022 Jun), 2102742.
- [19] H.Y. Xiang, Y.Q. Li, S.S. Meng, C.S. Lee, L.S. Chen, J.X. Tang, Extremely efficient transparent flexible organic light-emitting diodes with nanostructured composite electrodes, *Adv. Opt. Mater.* 6 (2018).
- [20] L.H. Xu, Q.D. Ou, Y.Q. Li, Y.B. Zhang, X.D. Zhao, H.Y. Xiang, J.D. Chen, L. Zhou, S. T. Lee, J.X. Tang, Microcavity-free broadband light outcoupling enhancement in flexible organic light-emitting diodes with nanostructured transparent metal-dielectric composite electrodes, *ACS Nano* 10 (2016) 1625–1632.
- [21] Y.L. Zhu, Y.Y. Hao, S.Q. Yuan, F. Zhang, Y.Q. Miao, Y.X. Cui, Z.F. Li, H. Wang, B. S. Xu, Improved light outcoupling of organic light-emitting diodes by randomly embossed nanostructure, *Synth. Met.* 203 (2015) 200–207.
- [22] X.M. Peng, C.H. Yeh, S.F. Wang, J. Yan, S.F. Gan, S.J. Su, X.W. Zhou, Y.X. Zhang, Y. Chi, Near-infrared OLEDs based on functional pyrazinyl azolate Os(II) phosphors and deuteration, *Adv. Opt. Mater.* (2022), <https://doi.org/10.1002/adom.202201291>.
- [23] K. Das Patel, F.S. Juang, H.X. Wang, C.Z. Jian, J.Y. Chen, Quantum dot-based white organic light-emitting diodes excited by a blue OLED, *Appl. Sci.-Basel* 12 (2022).
- [24] I.N.S. Manoj, D. Barah, S. Sahoo, J. Bhattacharyya, D. Ray, Enhancing the efficiency of red TADF OLED by optimizing the guest-host matrix and charge balance engineering, *Synth. Met.* 270 (2020).
- [25] T. Zhou, Y. Qian, H.J. Wang, Q.Y. Feng, L.H. Xie, W. Huang, Recent advances in substituent effects of blue thermally activated delayed fluorescence small molecules, *Chim. Sin.* 79 (2021) 557–574.
- [26] C.J. Wu, J.S. Miao, L. Wang, Y.M. Zhang, K. Li, W.G. Zhu, C.L. Yang, Red and near-infrared emissive palladium(II) complexes with tetradentate coordination framework and their application in OLEDs, *J. Chem. Eng.* 446 (2022).
- [27] J.S. Siegel, T.J. Seiders, From bowls to saddles, *Chem. Brit.* 31 (1995) 313–318.
- [28] T. Hensel, N.N. Andersen, M. Plesner, M. Pittelkow, Synthesis of heterocyclic [8] circulenes and related structures, *Synlett* 27 (2016) 498–525.
- [29] D. Cagardová, J.n. Matúška, P. Poliak, V.r. Lukeš, Design of novel generations of planar sunflower molecules: theoretical comparative study of electronic structure and charge transport characteristics, *J. Phys. Chem. C* 123 (2019) 22752–22766.
- [30] H. Christoph, J. Grunenberg, H. Hopf, I. Dix, P.G. Jones, M. Scholtissek, G. Maier, MP2 and DFT calculations on circulenes and an attempt to prepare the second lowest benzolog,[4] circulene, *Chem.–Eur. J.* 14 (2008) 5604–5616.
- [31] Z. Ullah, H.J. Kim, S. Jang, Y.S. Mary, H.W. Kwon, DFT study of 6-amino-3-(1-hydroxyethyl) pyridine-2,4-diol (AHP) adsorption on Coronene, *J. Mol. Liq.* 360 (2022).
- [32] S.S. Manna, B. Pathak, Pyrrolidinium-based organic cation (BMP)-Intercalated organic (coronene) anode for high-voltage dual-ion batteries: a comparative study with graphite, *J. Phys. Chem. C* 126 (2022) 9264–9274.
- [33] J.M. Warman, M.P. de Haas, G. Dicker, F.C. Grozema, J. Piris, M.G. Debije, Charge mobilities in organic semiconducting materials determined by pulse-radiolysis time-resolved microwave conductivity: π -bond-conjugated polymers versus π - π -stacked discotics, *Chem. Mater.* 16 (2004) 4600–4609.
- [34] X. Zhang, X. Jiang, K. Zhang, L. Mao, J. Luo, C. Chi, H.S.O. Chan, J. Wu, Synthesis, self-assembly, and charge transporting property of contorted tetrabenzocoronenes, *J. Org. Chem.* 75 (2010) 8069–8077.
- [35] N.N. Karaush, G.V. Baryshnikov, V.A. Minaeva, H. Ågren, B.F. Minaev, Recent progress in quantum chemistry of hetero [8] circulenes, *Mol. Phys.* 115 (2017) 2218–2230.
- [36] J.C. Sorli, P. Friederich, B. Sanchez-Lengeling, N.C. Davy, G.O.N. Ndjawa, H. L. Smith, X. Lin, S.A. Lopez, M.L. Ball, A. Kahn, Coronene derivatives for transparent organic photovoltaics through inverse materials design, *J. Mater. Chem. C* 9 (2021) 1310–1317.
- [37] A.L. Appleton, S.M. Brombosz, S. Barlow, J.S. Sears, J.-L. Bredas, S.R. Marder, U. H. Bunz, Effects of electronegative substitution on the optical and electronic properties of acenes and diazaacenes, *Nat. Commun.* 1 (2010) 91.
- [38] G.V. Baryshnikov, R.R. Valiev, N.N. Karaush, V.A. Minaeva, A.N. Sinelnikov, S. K. Pedersen, M. Pittelkow, B.F. Minaev, H. Ågren, Benzoannelated aza-, oxa- and azaoxa [8] circulenes as promising blue organic emitters, *Phys. Chem. Chem. Phys.* 18 (2016) 28040–28051.
- [39] G. Sarki, B. Tüzün, D. Ünlütür, H. Kantekin, Synthesis, characterization, chemical and optical activities of 4-(4-methoxyphenethyl)-5-benzyl-2-hydroxy-2H-1, 2, 4-triazole-3 (4H)-one phthalocyanine derivatives, *Inorg. Chim. Acta.* (2022), 121113.
- [40] A.A. Youssef, S.M. Bouzzine, Z.M.E. Fahim, I. Sidir, M. Hamidi, M. Bouachrine, Designing Donor-Acceptor thienopyrazine derivatives for more efficient organic photovoltaic solar cell: a DFT study, *Physica B* 560 (2019) 111–125.
- [41] R. Omidyar, M. Abbasi, G. Azimi, Photophysical and optoelectronic properties of a platinum(II) complex and its derivatives, designed as a highly efficient OLED emitter: a theoretical study, *Int. J. Quant. Chem.* 119 (2019).
- [42] P. Rezaee, H.R. Naeij, Graphenylene-1 membrane: an excellent candidate for hydrogen purification and helium separation, *Carbon* 157 (2020) 779–787.
- [43] W.R. Zhai, M.H. Wang, S. Liu, S.Y. Xu, H. Dong, L. Wang, S.X. Wei, Z.J. Wang, S. Y. Liu, X.Q. Lu, Theoretical Investigation on Two-Dimensional Conjugated Aromatic Polymer Membranes for High-Efficiency Hydrogen Separation: the Effects of Pore Size and Interaction, *Sep Purif Technol.* 2022, p. 299.
- [44] M.M. Samy, I.M.A. Mekhemer, M.G. Mohamed, M.H. Elsayed, K.H. Lin, Y.K. Chen, T.L. Wu, H.H. Chou, Conjugated microporous polymers incorporating Thiazolo [5,4-d]thiazole moieties for Sunlight-Driven hydrogen production from water, *J. Chem. Eng.* 446 (2022).
- [45] J. Bachmann, A. Helbig, M. Crumbach, I. Krummenacher, H. Braunschweig, H. Helten, Fusion of Aza- and Oxadiborepins with Furans in a Reversible Ring-Opening Process Furnishes Versatile Building Blocks for Extended Pi-Conjugated Materials, *Chem-Eur J*, 2022.
- [46] Z.R. Chen, Y.J. Zhang, Y. Li, W.H. Yu, Charge transport properties in functionalized triphenylene and coronene derivatives: a density functional study using different functionals, *Mol. Cryst. Liq. Cryst.* 722 (2021) 95–109.
- [47] G.T. Oyeniyi, I.A. Melchakova, L.A. Chernozatonskii, P.V. Avramov, Nanodiamond islands confined between two graphene sheets as perspective 2D quantum materials, *Carbon* 196 (2022) 1047–1053.
- [48] M.J. Frisch, G.W. Trucks, H.B. Schlegel, G.E. Scuseria, M.A. Robb, J.R. Cheeseman, G. Scalmani, V. Barone, G.A. Petersson, H. Nakatsuji, X. Li, M. Caricato, A. V. Marenich, J. Bloino, B.G. Janesko, R. Gomperts, B. Mennucci, H.P. Hratchian, J. V. Ortiz, A.F. Izmaylov, J.L. Sonnenberg, Williams, F. Ding, F. Lipparini, F. Egidi, J. Goings, B. Peng, A. Petrone, T. Henderson, D. Ranasinghe, V.G. Zakrzewski, J. Gao, N. Rega, G. Zheng, W. Liang, M. Hada, M. Ehara, K. Toyota, R. Fukuda, J. Hasegawa, M. Ishida, T. Nakajima, Y. Honda, O. Kitao, H. Nakai, T. Vreven, K. Throssell, J.A. Montgomery Jr., J.E. Peralta, F. Ogliaro, M.J. Bearpark, J. J. Heyd, E.N. Brothers, K.N. Kudin, V.N. Staroverov, T.A. Keith, R. Kobayashi, J. Normand, K. Raghavachari, A.P. Rendell, J.C. Burant, S.S. Iyengar, J. Tomasi, M. Cossi, J.M. Millam, M. Klene, C. Adamo, R. Cammi, J.W. Ochterski, R.L. Martin, K. Morokuma, O. Farkas, J.B. Foresman, D.J. Fox, Gaussian 16, Rev. C.01, Wallingford, CT, 2016.
- [49] G. te Velde, F.M. Bickelhaupt, E.J. Baerends, C.F. Guerra, S.J.A. Van Gisbergen, J. G. Snijders, T. Ziegler, Chemistry with ADF, *J. Comput. Chem.* 22 (2001) 931–967.
- [50] A.D. Bochevarov, E. Harder, T.F. Hughes, J.R. Greenwood, D.A. Braden, D. M. Philipp, D. Rinaldo, M.D. Halls, J. Zhang, R.A. Friesner, Jaguar: a high-

- performance quantum chemistry software program with strengths in life and materials sciences, *Int. J. Quant. Chem.* 113 (2013) 2110–2142.
- [51] X. Li, B. Minaev, H. Ågren, H. Tian, Density functional theory study of photophysical properties of iridium (III) complexes with phenylisoquinoline and phenylpyridine ligands, *J. Phys. Chem. C* 115 (2011) 20724–20731.
- [52] R.A. Marcus, Electron-transfer reactions in chemistry - theory and experiment, *Rev. Mod. Phys.* 65 (1993) 599–610.
- [53] U. Daswani, U. Singh, P. Sharma, A. Kumar, From molecules to devices: a DFT/TD-DFT study of dipole moment and internal reorganization energies in optoelectronically active aryl azo chromophores, *J. Phys. Chem. C* 122 (2018) 14390–14401.
- [54] S.S. Tang, J.P. Zhang, Rational design of organic asymmetric donors D1-A-D2 possessing broad absorption regions and suitable frontier molecular orbitals to match typical acceptors toward solar cells, *J. Phys. Chem. A* 115 (2011) 5184–5191.
- [55] A. Irfan, A. Kalam, A.R. Chaudhry, A.G. Al-Sehemi, S. Muhammad, Electro-optical, nonlinear and charge transfer properties of naphthalene based compounds: a dual approach study, *Optik* 132 (2017) 101–110.
- [56] R.G. Pearson, Chemical hardness and bond dissociation energies, *J. Am. Chem. Soc.* 110 (1988) 7684–7690.
- [57] Y. Tao, K. Yuan, T. Chen, P. Xu, H. Li, R. Chen, C. Zheng, L. Zhang, W. Huang, Thermally activated delayed fluorescence materials towards the breakthrough of organoelectronics, *Adv. Mater.* 26 (2014) 7931–7958.
- [58] R.A.K. Yadav, D.K. Dubey, S.-Z. Chen, T.-W. Liang, J.-H. Jou, Role of molecular orbital energy levels in OLED performance, *Sci Rep-Uk* 10 (2020) 1–15.
- [59] A. Lukyanov, C. Lennartz, D. Andrienko, Amorphous films of tris (8-hydroxyquinolinato) aluminium: force-field, morphology, and charge transport, *Phys. Status Solidi* 206 (2009) 2737–2742.
- [60] N.E. Gruhn, D.A. da Silva Filho, T.G. Bill, M. Malagoli, V. Coropceanu, A. Kahn, J.-L. Brédas, The vibrational reorganization energy in pentacene: molecular influences on charge transport, *J. Am. Chem. Soc.* 124 (2002) 7918–7919.
- [61] U. Daswani, U. Singh, P. Sharma, A. Kumar, From molecules to devices: a DFT/TD-DFT study of dipole moment and internal reorganization energies in optoelectronically active aryl azo chromophores, *J. Phys. Chem. C* 122 (2018) 14390–14401.
- [62] A.A. Youssef, S.M. Bouzzine, Z.M.E. Fahim, İ. Sıdır, M. Hamidi, M. Bouachrine, Designing Donor-Acceptor thienopyrazine derivatives for more efficient organic photovoltaic solar cell: a DFT study, *Phys. B Condens. Matter* 560 (2019) 111–125.
- [63] S.G. Patel, R.M. Vala, P.J. Patel, D.B. Upadhyay, V. Ramkumar, R.L. Gardas, H. M. Patel, Synthesis, crystal structure and in silico studies of novel 2, 4-dimethoxy-tetrahydropyrimido [4, 5-b] quinolin-6 (7 H)-ones, *RSC Adv.* 12 (2022) 18806–18820.